

# Detection of gas pockets in dendritic wastewater mains

Ivo Pothof, <sup>1), 2)</sup>

Francois Clemens <sup>2)</sup>

<sup>1)</sup> Department of Industrial Flow Technology,  
Deltares | Delft Hydraulics, The Netherlands

<sup>2)</sup> Department of Water Management, section Sanitary Engineering,  
Delft University of Technology, The Netherlands

## ABSTRACT

Wastewater pressure mains are subject to gas pockets in declining sections. These gas pockets cause unforeseen head losses and capacity reduction. Lubbers and Clemens (Lubbers 2005) have investigated the potential of transient pressures to detect the location of gas pockets in wastewater mains. The method is based on an analysis of the Fourier transform of a measured transient pressure signal and predicts the location of a single gas pocket in a simple pipeline with sufficient accuracy. The method has been verified in a 650 m long PVC pipeline ( $\varnothing 235$  mm). This paper proposes an extension to the gas pocket detection method, such that the gas pocket volume is predicted as well. Furthermore, a number of issues on the practical applicability are discussed. The extended detection method has been verified with simulations of a dendritic system. The numerical results indicate that the extended detection method can be tested in practice.

**keywords:** detection gas pockets, pressure surges, wastewater pipelines, dendritic systems.

## Nomenclature

<i>A</i>	Pipe cross section [m <sup>2</sup> ]
<i>C</i>	thermodynamic constant [J * m <sup>3k-3</sup> ]
<i>c</i>	Pressure wave propagation speed [m/s]
<i>D</i>	Internal pipe diameter [m]
<i>E</i>	Pipe wall Young's modulus, modulus of elasticity [Pa]
<i>e</i>	Wall thickness [m]
<i>f</i>	Pipe frequency [Hz]
<i>g</i>	Gravitational acceleration [m <sup>2</sup> /s]
<i>H</i>	Head, function of location and time [m]
<i>K</i>	Liquid bulk modulus [Pa]
<i>k</i>	polytropic coefficient [-]
<i>L</i>	System length [m]
<i>P</i>	Pipe period – characteristic period [s]

$P_0$	oscillation period [s]
$p$	Absolute pressure [Pa abs]
$s$	Axial location [m]
$\Delta s$	Pipe strain [m]
$t$	Time [s]
$V$	main line volume [m <sup>3</sup> ]
$v$	Cross section average velocity [m/s]
$v'$	Dimensionless velocity [-]
$\rho$	Liquid density [kg/m <sup>3</sup> ]
$\mathcal{A}_0$	Elastic storage of main line without gas pockets
$\mathcal{A}_1$	Elastic storage of gas pockets

#### *Subscripts*

0	Reference situation (without gas pockets)
1	Including gas pockets
i	Initial, steady state situation
f	Final state after the transient
g	first gas pocket

## 1 Introduction

One of main causes of a capacity reduction is the presence of gas pockets in declining pipe sections. These gas pockets cannot be easily transported and become an obstruction for the wastewater flow.

The Capwat I project (2003 – 2006) has proven that the existing design approach, based on Kent's formula for mitigation of gas pockets (Kent 1952), is not valid (Lubbers 2007). Kent's formula for the required dimensionless velocity ( $v' = v/\sqrt{gD}$ ) is too optimistic for declining angles smaller than 25°. Therefore, capacity reducing gas pockets reside in many inverted siphons of wastewater mains.

During normal operation, a maintenance engineer or an operator would like to have practical and simple tools at his/her disposal to determine which processes are causing a certain capacity reduction. Knowledge about the most likely cause of the capacity reduction — gas pockets or scaling — supports the decision about the most efficient measure to be taken.

This paper proposes a gas pocket detection method that distinguishes gas pockets from other causes of capacity reduction. The proposed detection method locates a gas pocket and assesses the total gas pocket volume in a dendritic (wastewater) system. The detection method takes a number of practical requirements into account.

Section 2 summarizes the current status of literature. Section 3 details an existing method to locate a single gas pocket from a frequency analysis. Section 4 derives an equation for the total gas pocket volume as a function of a measured frequency shift. Section 5 describes the extended detection method and various tests, illustrating the feasibility of the approach, are presented in section 6. Finally, section 7 presents conclusions and recommendations.

## 2 Literature overview

The application of fluid transients for system or flow characterisation has been investigated since the 1990s. These investigations focus on leak detection in oil transportation lines (Liou 1993), leak detection in water mains (Brunone 1999; Ferrante and Brunone 2003) and distribution networks (Liggett and Chen 1994), multiphase flow measurement (Gudmundsson 1999) and the determination of the valve status and identification of pipe blockages (Stephens 2004).

Stoianov et al. identified a number of practical limitations and concluded that the use of transient and inverse transient analysis (ITA) would be “unlikely to have any value for the water industry” (Stoianov 2003). Covas et al. have performed field tests to assess the practical applicability of transient (pressure) signals for the detection of leaks (Covas 2004). Covas concludes that both time analysis and ITA were successful in the detection and location of leaks of a ‘reasonable’ size. Stephens et al. have performed field tests to assess the practical applicability for the detection of leaks, air pockets and pipe blockage (Stephens, Lambert et al. 2004). Stephens et al. conclude that ITA was successful in detecting an air pocket and less successful in detecting pipe blockage and leaks. ITA is a powerful tool to tune uncertain system parameters to a measured transient response, but ITA requires quite some specialist knowledge about transient solvers and efficient search strategies to adjust the uncertain parameters. The literature, exploring ITA, focuses on very fast operations (i.e.  $\ll$  pipe period), which is impractical or, at least, requires careful preparation.

Lubbers and Clemens (Lubbers 2005) have investigated the potential of transient pressures to detect the location of gas pockets in sewage water mains with a simpler method. Their method is based on an analysis of the Fourier transform of a measured pressure transient. This method predicts the location of a single gas pocket in a single pipeline with sufficient accuracy. The method is briefly summarized in section 3. The method has been verified in a 630 m long test pipeline ( $\varnothing 235$  mm). The authors of this paper believe that air pockets can be detected more easily than leaks or blockages, because the presence of air pockets directly influences the wave propagation and the pipeline period, while leaks and blockages only create reflections, that must have sufficient magnitude to be discriminated from system noise.

### 3 Gas pocket detection by frequency analysis

A pressure transient, induced by a rapid valve closure or pump speed reduction, reflects on the other side of a single pipeline and returns to the source, reflects again and leads to a periodic pressure time series at each location in the pipeline. The period of the oscillation depends on the type of boundary conditions and equals one or two pipeline periods ( $P$ ), where the pipeline period is defined in accordance with Thorley (Thorley 2004) as:

$$P = \frac{2L}{c} \quad (1)$$

The oscillation period,  $P_o$ , equals the pipeline period, if the pipeline boundaries are both open (i.e. tanks or reservoirs) or both closed (i.e. closed valves). The oscillation period equals  $2P$ , if one boundary is open and the other boundary is closed. The oscillation frequency,  $f_0 = P_o^{-1}$  [Hz], is the base frequency in the Fourier transform of a pressure time series, because the Fourier transform shows the frequency content of a time signal. Normally, the Fourier transform shows smaller peaks at integer factors of the base frequency – so-called higher harmonics. Lubbers has derived Figure 1 from pump ramp down operations in a 630 m test pipeline with a single gas pocket of known volume, trapped in a vertical stand pipe at different locations from the pump. The pressure traces, from which Figure 1 was derived, were measured 520 m from the pump, while the gas pocket trapped at 394 m from the pump. Figure 1 shows two higher harmonics in the Fourier transform of the pressure trace without gas pockets (legend *air column = 0 cm*).

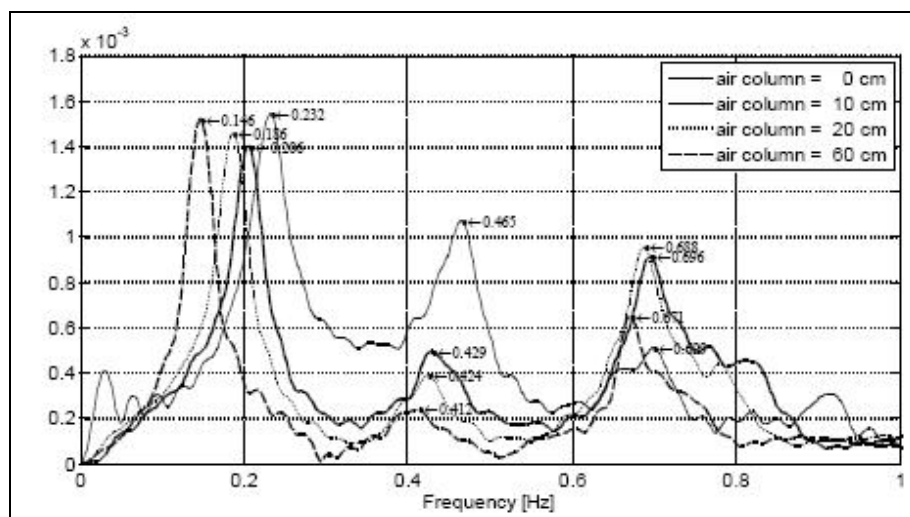


Figure 1: Fourier transforms of measured transient pressures in 630 m test pipeline

If a gas pocket is present, somewhere in a single pipeline, then the pressure transient will reflect on the gas pocket, because of the large compressibility of the gas pocket. The early reflection generates a shorter oscillation period and, therefore, a higher frequency in the frequency domain. Lubbers (Lubbers 2007) has exploited this higher frequency to estimate the location of a gas pocket; see e.g. the peaks around a frequency of 0.42 Hz in Figure 1, which are not second harmonics of the base frequencies around 0.18 Hz.

Lubbers' detection method (Lubbers 2005) is extended to predict the gas pocket volume, because knowledge about the gas volume is required to assess the risk of a sudden capacity reduction at increased flow rates. The method is further extended to handle branched systems, possibly including air vessels, and systems with multiple gas pockets, because these are more common in practice.

#### 4 Gas pocket volume and frequency drop

The frequency drop due to a gas pocket will be fully understood after some properties of the wave speed have been discussed. The wave speed appears in the continuity equation.

$$\frac{\partial v}{\partial s} + \frac{g}{c^2} \frac{\partial H}{\partial t} = 0 \quad (2)$$

where

$$\frac{1}{c^2} = \rho \left( \frac{1}{K} + \frac{1}{A} \frac{dA}{dp} + \frac{1}{\Delta s} \frac{d\Delta s}{dp} \right) = \rho \left( \frac{1}{K} + \frac{D}{eE} \right) \quad (3)$$

(the symbols are explained in the Nomenclature)

The more fundamental expression of the wave speed shows that the wave speed represents all possible internal elastic storage contributions, i.e. elastic storage due to fluid compressibility and radial and axial pipe expansion. The larger the elastic storage, the smaller the wave speed; for this reason the wave speed in flexible plastic pipes is significantly smaller than in steel pipes.

A gas pocket is an extra source of elastic storage that reduces the average wave speed in the pipeline and consequently reduces the base frequency. The larger the gas pocket, the larger the storage and the smaller the base frequency. Hence the reduction of the base frequency potentially predicts the gas pocket volume.

Let us now establish the relation between the total gas volume in the main line of a dendritic system and the average wave speed in the main line. The main line of a dendritic system comprises the series of pipes from the main pumping station to the downstream boundary. The elastic storage is conveniently expressed as a storage area, which is directly derived from the continuity equation:

$$\mathcal{A}_0 = \frac{\Delta V}{\Delta H} = \frac{g \cdot V}{c_0^2} \quad (4)$$

The subscript 0 refers to the reference condition without gas pockets and subscript 1 will refer to a condition including one or more gas pockets in the main line. The storage area, associated with an initial gas pocket of volume  $V_i$ , is derived from the following thermodynamic relation:

$$p \cdot V^k = C \quad (5)$$

After some algebraic manipulation and a first order Taylor expansion, the gas pocket storage area equals:

$$\mathcal{A}_1 = \frac{\Delta V}{\Delta H} = \frac{\rho \cdot g \cdot V_i}{k \cdot p_f} \quad (6)$$

Now the total elastic storage area in the system with gas pockets is simply the sum of all elastic storage areas, yielding an average wave speed,  $c_1$ , in the main line, which obeys the following expression:

$$\frac{1}{c_1^2} = \frac{1}{c_0^2} + \frac{\rho \cdot V_i}{k \cdot p_f \cdot V} \quad (7)$$

The average wave speeds in equation (7) correspond to certain base frequencies in the frequency domain. The base frequency of the main line is determined from the length of the main line, the average wave speed and the boundary type, as discussed above:

Different boundaries  $f = \frac{c}{4L} \quad (8)$

Similar boundaries  $f = \frac{c}{2L} \quad (9)$

The total gas pocket volume is now computed from a certain frequency reduction by combining equation (7) and (8) or (9), yielding:

Different boundaries  $V_i = \frac{k \cdot p_f \cdot V}{16L^2 \cdot \rho} \left( \frac{1}{f_1^2} - \frac{1}{f_0^2} \right) \quad (10)$

Similar boundaries  $V_i = \frac{k \cdot p_f \cdot V}{4L^2 \cdot \rho} \left( \frac{1}{f_1^2} - \frac{1}{f_0^2} \right) \quad (11)$

These equations couple the base frequencies, such that the observed frequency reduction determines the total gas pocket volume, irrespective of the number of individual gas pockets in the pipeline. The presence of the branches and the branch flows are reflected in the base frequency of the reference transient,  $f_0$ . The higher frequency response will still predict the location of the first gas pocket. If gas is distributed along the pipeline, then the higher frequency peak will be absent, which will be demonstrated in a numerical example in section 6.3. Section 5 will first detail the extended gas pocket detection method and discuss practical aspects of the detection method.

## 5 Extended detection method

It is assumed that the main line is easily identified in a dendritic wastewater transportation system. One or more branches link onto the main line. The dendritic system has a base frequency, depending on the properties of the main line and the branches in a complicated way. This base frequency cannot be accurately assessed from analytical calculations. Now some computer power is exploited by modelling a reference case without gas pockets and running a suitable harmless transient. The simulated reference transient must be harmless, because the same transient must be induced in the real system in order to detect the presence of gas pockets. The simulated and measured signals are Fourier transformed, using the Fast Fourier Transform (FFT), to determine the frequency content of the signals. Before equation (10) or (11) can be applied to compute the total gas pocket volume, the parameters must be estimated, which is not trivial in a dendritic system. These parameters – polytropic coefficient and final gas pressure – will be discussed in the following paragraphs.

The polytropic coefficient,  $k$ , is in fact not a real constant, but this parameter depends on transient heat fluxes to and from the gas pocket and the gas pocket composition, which is hardly predictable in practice. Gas pockets may include methane, carbon dioxide, hydrogen sulfide and nitrogen in varying concentrations. A polytropic coefficient of 1.0 corresponds with isothermal gas pocket behaviour, a value of 1.4 corresponds with adiabatic behaviour, if the gas pocket composition is similar with air. If the gas pockets have a large methane content, then the maximum value reduces to 1.35. A reasonable estimate of the polytropic coefficient is 1.2. A sensitivity analysis over the range of possible values of the polytropic coefficient provides insight in its impact on the gas pocket volume prediction.

The pressure parameter,  $p_f$ , represents the absolute final pressure in the gas pocket(s) at the end of the reference scenario. The reference scenario provides detailed information on all final pressures along the main line. If the system includes considerable elevation differences, then the final pressures may differ significantly along the line.

The second frequency peak of the measured pressure can be used to locate the gas pocket. The method is illustrated in Figure 2 and elaborated hereafter. Suppose that the transient has been generated by a pump trip that has led to check valve closure. Furthermore, suppose that the pressure, measured downstream of the check valve, reveals a base frequency  $f_1$  and a second frequency peak at  $f_2$ , as illustrated in Figure 2. The subsystem between the check valve and the first gas pocket, which is responsible for generating the frequency peak at  $f_2$ , has two different boundaries; namely the closed check valve and the ‘open’ gas pocket. Therefore, equation (8) must be applied to obtain the location of the first gas pocket,  $L_g$ .

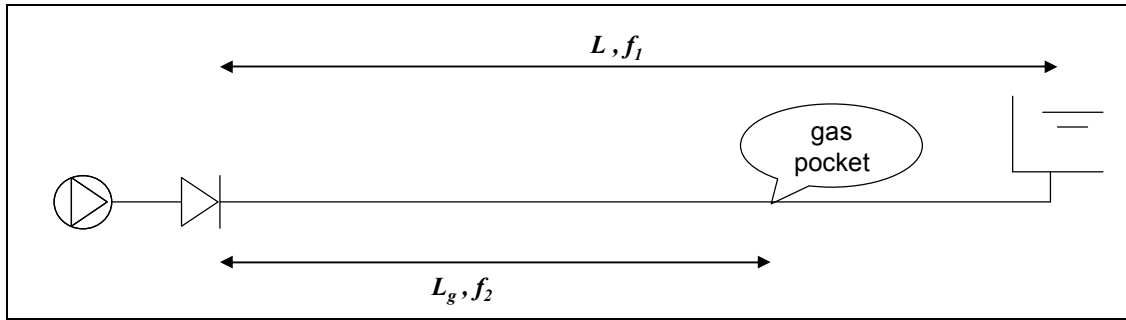


Figure 2: Method to determine first gas pocket location from measured frequency content

Once the location of the first gas pocket is known, the pressure parameter,  $p_f$ , can be set to the absolute simulated pressure at a distance  $L_g$  from the pumping station, at the end of the reference scenario. After all parameters have been set, the total gas volume can be estimated from equation (10) or (11); the result is the total gas volume, from which a fraction is present around location  $L_g$ .

The extended detection method is summarised in the following steps:

1. Build a simulation model of the pressurised dendritic wastewater system, and include sufficient information for transient simulations. This model is preferably validated against field data without gas pockets in the system in order to verify that the simulation model captures the reference frequency correctly, which mainly requires correct information on the system lengths and pipe materials.
2. If the transient is initiated from a pumping station, then all anti-surge devices must be disabled in the model – and later in the field as well. The impact of the transient event without anti-surge devices must be verified to prevent damage to the system.
3. Determine in the simulation model which transient can be imposed on the system (e.g. downstream valve closure, pump trip or closure of discharge valve) without violating the incidental pressure criteria. Cavitation should be prevented, because cavities generate similar reflections as gas pockets<sup>\*)</sup>. This is the reference case.
4. Install a pressure transducer in the main line at an accessible location, where pressure oscillations will occur during the transient, which can be verified in the reference case. Generally, the only above-ground piping is in the pumping station. In this case, the pumping station's check valves must close or the discharge valve must close and the pressure must be recorded downstream of these valves; otherwise the transducer will record the suction level shortly after the beginning of the transient event.

<sup>\*)</sup> The transient event must be balanced between two competing criteria. On one hand, the transient must be as strong as possible to maximise the information content in the pressure signal. On the other hand, the transient event should not cause cavitation, de-aeration or pipe damage. Rapid de-aeration in water starts at about 5 metres above vapour pressure.



5. Initiate the transient event in the real system and record the transient pressure. The sample frequency must be greater than 10 times the base frequency of the simulated system.
6. Extend the time series to the next integer power of 2 values with the average value of the complete time series. One reason for this step is to benefit from the most efficient implementation of the Fast-Fourier-Transform (FFT). A second reason is to improve the accuracy of the peak frequency; if the array is doubled in length, then the frequency resolution becomes twice as small. A third argument is that some tools, like Microsoft Excel, only support FFT arrays with this length requirement, because they only have implemented the most efficient FFT algorithm. The second argument is the most relevant, because the base frequency is relatively low and drops further if gas pockets are present. Some guidance is provided by the fact that the frequency resolution,  $\Delta f$ , equals  $1/T$ , where T is the covered time of the extended time series.
7. Determine the FFT of the measured pressure signal and the simulated pressure signal at the same location. The FFT routine is widely available in, for example, the default Data analysis Add-in from Microsoft Excel, in Matlab and in practically all other time series analysis packages. The FFT is a series of complex numbers with resolution  $\Delta f$ , from which the absolute values are further processed.
8. Plot the FFT arrays and determine the largest frequency in each array. Furthermore determine the second largest frequency in the measured array. The two measured frequencies should differ less than 1 order of magnitude. The largest frequency in the simulated FFT is  $f_0$ , the largest and second largest measured frequency are  $f_1$  and  $f_2$ , respectively.
9. Apply equation (8), if the boundary is closed, or equation (9), if the boundary is open, to obtain the location of a possible first gas pocket.
10. Determine the absolute final pressure,  $p_f$ , at this location from the reference simulation.
11. Apply equation (10) or (11) to obtain an estimate of the total gas volume.

The only parameters that have not been elaborated so far, are the applicable volume and characteristic length in equation (10) or (11). The predictability of the gas pocket location and total gas volume will be discussed in the feasibility test cases in section 6.

## 6 Feasibility of the extended detection method

As a first test of the practical applicability of the detection method, the method is applied to the single pipe system, from which the data is shown in Figure 2. The predicted location varies from 347 m to 362 m, while the real gas pocket location was 394 m. The predicted volume varied between 73% and 89% of the real volume. These results are considered practically relevant. The feasibility of the described detection method is further verified in a system with one side branch. The ‘measurements’ are generated

numerically with one, two and many gas pockets at unknown locations in the main line. All transient simulations have been performed with WANDA, version 3.60 (Deltares 1993 - 2008).

## 6.1 Reference transients and gas pocket transients

The key properties of the test system are listed in Table 1 and on the lay-out in Figure 3.

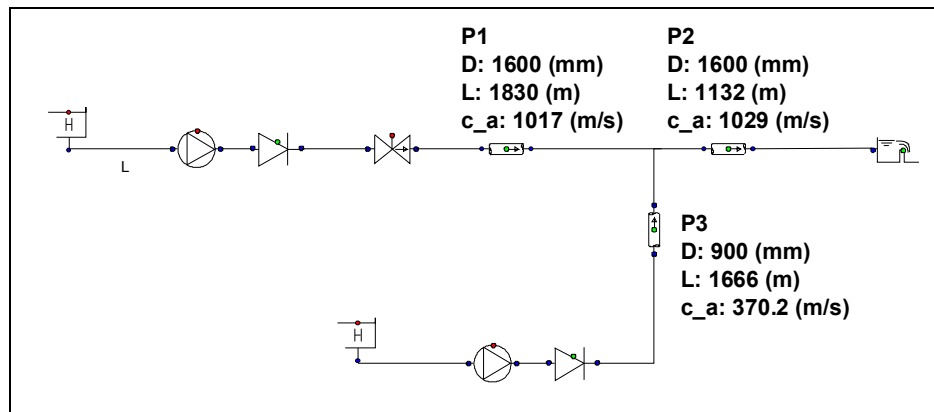


Figure 3: Lay-out of test system and relevant pipe properties (diameter, length, wavespeed)

Table 1: Overview of test system pipe properties

Pipe	Diameter [mm]	Length [m]	Volume [m <sup>3</sup> ]	Wave speed [m/s]	Pipeline period [s]
P1	1600	1830	3679	1017	3.6
P2	1600	1132	2276	1029	2.2
Total main	1600	2962	5955	1022	5.8
P3 (branch)	900	1666	1060	370	9.0

The operational conditions of the reference transients consist of the closure of the discharge valve from a suitable, harmless, steady state flow. The valve closure can be rapid (effective closure in 3 s) or slow (effective closure in 10 s); the pipeline period is 6.6 s. The initial velocity for the 3 s valve closure scenario is about 10% of the design velocity. The flow from the side branch is set to the design flow rate or to zero. These parameter combinations yield 4 different reference transients, which are summarized in Table 2 below.

Table 2: Overview of operational conditions of reference transients in test system

Reference cases	Initial velocity main [m/s]	Closure time [s]	Initial velocity side [m/s]
3s_side	0.18	3	1.7
3s_noside	0.18	3	0
10s_side	0.36	10	1.7
10s_noside	0.36	10	0

The simulated transient pressures, downstream of the discharge valve, in two reference cases are depicted in Figure 4 below. Figure 4 clearly illustrates that a branch in operation dampens the transient signal considerably. The damping will be stronger in practice, because unsteady friction has not been included in these simulations. It is anticipated that pressure damping due to unsteady friction does not affect the frequency analysis discussed in this paper. The frequency contents of the four reference transients are shown in Figure 5 hereafter, showing more pronounced peaks if the branch is switched off. The frequency peaks are listed in Table 3.

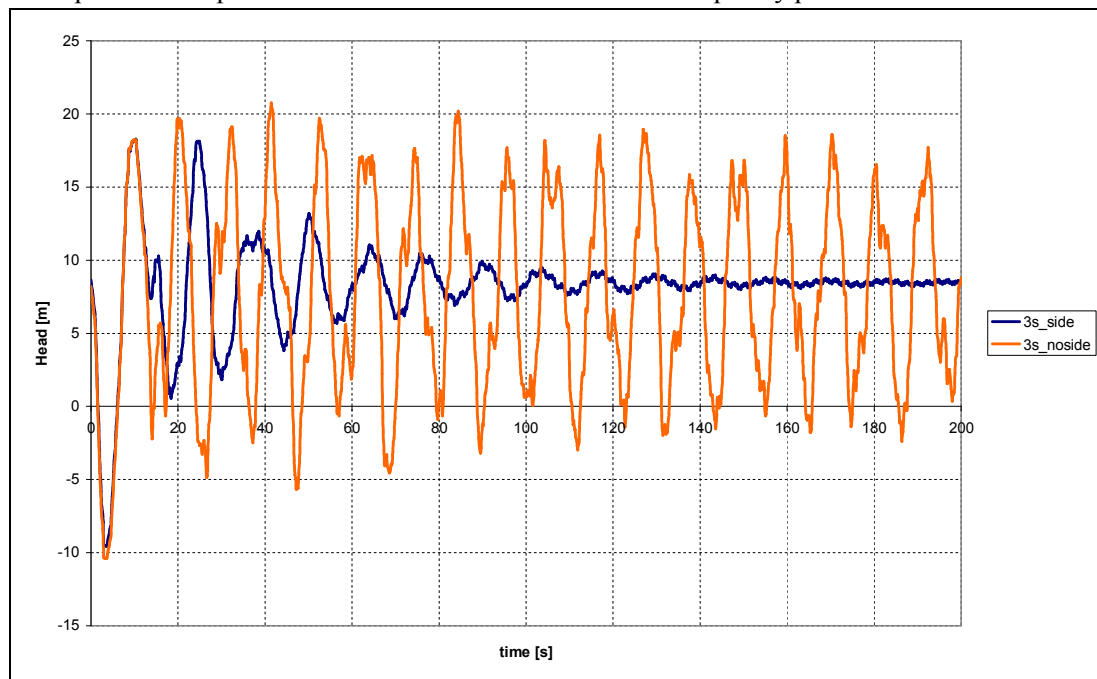


Figure 4: Transient pressures of 3 s valve closures (reference cases)

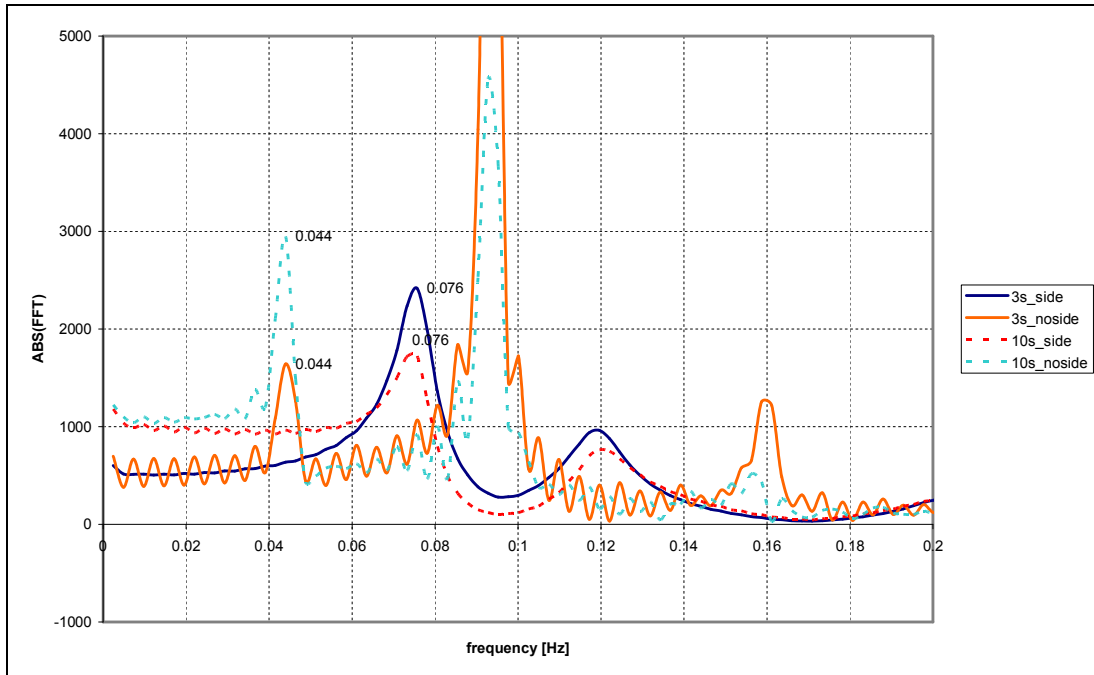


Figure 5: Frequency content of the reference transients (lowest frequencies)

Table 3: Frequency peaks of the reference scenarios

Scenario	Low frequency peak [Hz]	2 <sup>nd</sup> peak [Hz]
3s_side	0.076	0.120
3s_noside	0.044	0.093
10s_side	0.076	0.120
10s_noside	0.044	0.093

Inspection of Figure 5 immediately shows that the peak frequencies do not depend on the rate of the valve closure; even a 20 s valve closure shows the same frequency peaks. The frequency plot of the reference transients with the branch pumping station in operation shows two distinct peaks at 0.076 Hz and 0.12 Hz. If the branch pumping station is switched off, then the frequency plot shows the two largest peaks at 0.044 Hz and 0.093 Hz; these plots contain some other smaller peaks at 0.16 Hz, 0.24 Hz and 0.31 Hz. Section 6.2 discusses the different types of simulated gas pockets. The results are discussed in section 6.3.

## 6.2 Gas pocket transients

The transient pressure ‘measurements’ with gas pockets in the system have been generated numerically. The total gas pocket volume is 6 m<sup>3</sup> for all scenarios, which corresponds with 0.1% of the volume of the main pipeline. Gas pocket transients have

been generated with a single gas pocket, two smaller gas pockets or gas distributed along the main line. The detailed specifications of the gas pocket volume and location(s) are listed in Table 4. The individual gas pockets were modeled in WANDA with equation (5) that models the expansion and compression of the gas pockets correctly. The distributed gas was modeled with the same equation with an appropriate initial gas fraction; this equation was included at almost every internal calculation node along the pipeline.

Table 4: Specification of gas pockets

Scenario	# gas pockets [-]	volume [m <sup>3</sup> ]	location [m]	Notes
1gas	1	6	2035	location is 205 m after junction
2gas	2	3	1625	locations are 205 m before and after the junction
		3	2035	
distr.gas	distributed	6	distributed	equally distributed

Three different gas pocket specifications and 4 operational conditions yield a total of 12 cases with gas pockets. Furthermore 1 case has been included with reduced main diameter and increased wall roughness, in order to verify a clear distinction between gas pockets and other causes of capacity reduction. The wall roughness was increased by a factor 5 (to 1 mm) and the internal diameter was reduced by 5% (to 1520 mm). The operational condition was a 3 s valve closure with side flow. The roughness increase and diameter reduction caused a 50% increase of the hydraulic grade line and a marginal reduction of the flow rate of about 1%. The capacity reduction is marginal, because the discharge valve dominates the total head drop in the main line and the flow velocity in the common pipe after the junction is relatively small, because the main pumping station is running at 10% of its capacity only during these transients.

The gas pocket prediction results are discussed in 6.3.

### 6.3 Gas pocket predictions

As an example, the FFTs of all 3 s valve closure scenarios are shown in Figure 6. The scenarios with gas in the main line clearly show lower base frequencies, while the scenario with wall scaling (3s\_fric) shows the same base frequency as the reference scenario, which correctly indicates that the total gas volume is zero for the scenario with wall scaling (3s\_fric), according to equation (10). Furthermore, the frequency of the second peak of the scenario with two gas pockets at 0.18 Hz is greater than the frequency of the second peak of the one gas pocket scenario at 0.14 Hz, which is at least qualitatively consistent with the scenario parameters. Finally, the second peak of the distributed gas scenario is about one order of magnitude smaller than the first and occurs at the double frequency of the first peak, which indicates that this scenario has no clearly

located gas pocket and therefore the gas must be distributed. Table 5 summarizes the quantitative results.

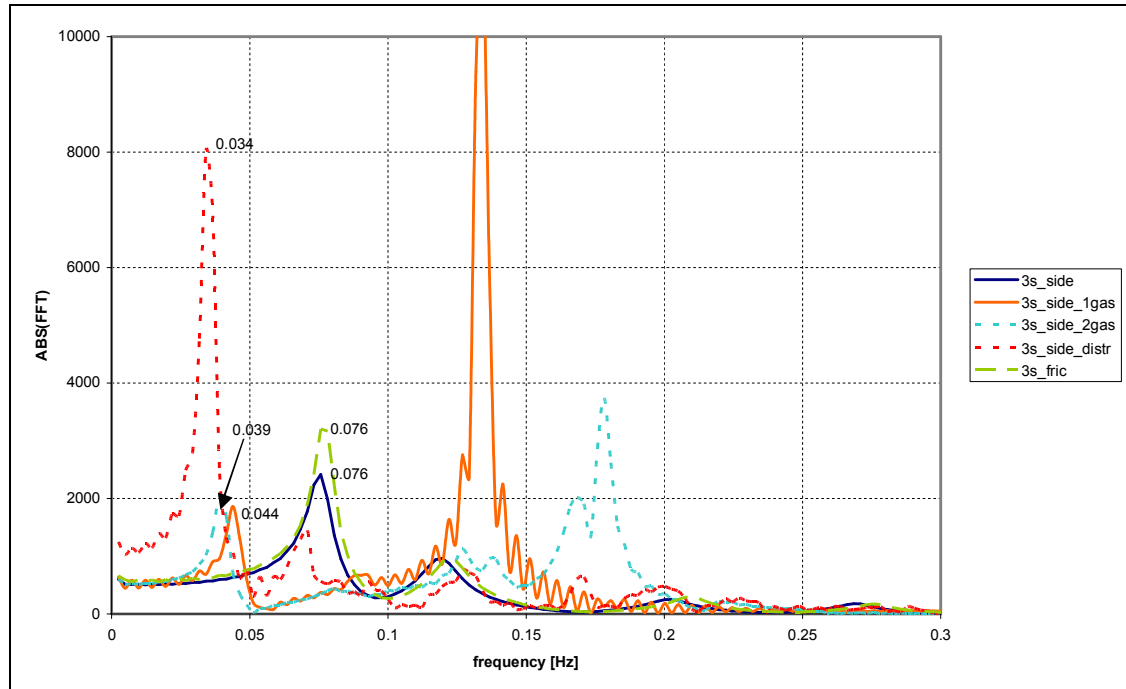


Figure 6: Frequency content of 3 s valve closure transients with branch flow

The following conclusions on the gas pocket location are drawn from Table 5. If the gas is concentrated in one pocket, then the predicted location is within 140 metres of the correct location (2035 m). If the gas is distributed in two gas pockets, then the location is underestimated by 200 metres. If the gas is distributed along the main line, then a second frequency peak is hardly visible; only the second harmonic frequency could be interpreted as such. In the latter case, the predicted location exceeds the pipe main length considerably (by more than 30% of the pipe main length). Hence, if a second frequency peak is not visible or the predicted length exceeds the total length and the predicted volume is non-zero, then the gas must be distributed along the main line.

If the manoeuvre is faster than the pipe period, then the second frequency peak, caused by the reflection on the gas pocket, is the largest peak in the FFT. This observation is illustrated in Figure 6, where the scenarios 3s\_side\_1gas (1 pocket) and 3s\_side\_2gas (2 pockets) have their maximum magnitudes at the second frequency peak. If, however, the manoeuvre is slower than the pipe period, then the maximum FFT values occur at the base frequency peak.

Table 5: Predicted gas pocket location and volume

Scenario	Low frequency peak [Hz]	2 <sup>nd</sup> peak [Hz]	Predicted location [m] (actually at 1625 m and/or 2035 m)	Predicted volume [m <sup>3</sup> ] (actually 6 m <sup>3</sup> )	Remarks
3s_side_1gas	0.0439	0.1318	1940	3.5	
3s_side_2gas	0.0391	0.1782	1430	4.8	
3s_side_distr	0.0366	N/A	N/A	5.8	
3s_fric	0.0757	0.1196	2140	0	
10s_side_1gas	0.0439	0.1318	1940	3.4	
10s_side_2gas	0.0391	0.1782	1430	4.8	two other peaks present
10s_side_distr	0.0342	0.0708	N/A	5.7	
<b>No side flow scenarios</b>					
3s_1gas	0.0350	0.1343	1900	3.0	
3s_2gas	0.0342	0.1782	1430	3.3	
3s_distr	0.0317	0.0635	4020	4.7	2 <sup>nd</sup> peak is 2 <sup>nd</sup> harmonic
10s_1gas	0.0342	0.1343	1900	3.3	
10s_2gas	0.0317	0.1782	1430	4.6	
10s_distr	0.0293	0.0610	4190	6.3	

The following conclusions on the gas pocket volume are drawn from Table 5. The scenario, in which the capacity reduction was caused by a diameter reduction and pipe roughness increase, correctly shows a total gas volume of 0 m<sup>3</sup>, because the base frequency equals the base frequency of the reference scenario. The total gas volume is more accurately predicted, if the gas volume is more distributed along the line. The predicted gas volume error is about 50%, if there is only one gas pocket in the pipeline, and better than 20% if the gas is distributed along the line. Hence the order of magnitude of the total gas pocket volume is predicted reasonably well. The prediction results are not significantly better for the scenarios with a stationary flow from the branch as was anticipated in section 6.1. The predictions of the fast closure scenarios are as good as the predictions of the slow closure scenarios.

## 7 Conclusions and recommendations

### 7.1 Conclusions

A relatively simple gas pocket detection method, compared to ITA, has been described and its feasibility has been addressed. The detection method investigates the frequency content of a measured or computed reference transient pressure signal without gas pockets and compares this frequency content with the frequency content of the measured transient pressure signal from the system, which may contain one or more gas pockets. The proposed method predicts both location and total gas volume in the main line. The feasibility of the method has been verified numerically in a test system with one large branch. The feasibility investigation has shown that the location can be predicted with an error smaller than 200 m, while the length of the wastewater main is about 3000 m. The total volume prediction differs less than 50% of the actual gas volume, with a tendency to underestimate the volume. It is concluded from this limited investigation that the proposed detection method has the potential to estimate the location of the first gas pocket and the total gas volume with sufficient accuracy for practical applicability.

If the transient scenarios are developed in such a way that the valves in the main pumping station close, then the transient pressure can be measured simply in the main pumping station downstream of the closing (check) valve, which is generally a location with easy access.

Despite the fact that less energy is dissipated, if the branch is switched off, the frequency plot with the branch in operation contains sufficient information for the detection method. Hence, the branch pumping stations can be operated normally during a transient detection test, initiated from the main pumping station. This investigation does not conclude that certain operational conditions for the branch pumping stations are recommended or required.

The duration of the transient event is not critical for the quality of the predictions. The 3 s operations and 10 s (or 20 s) operations yield similar results, while the pipeline period without gas pockets is 6.6 s. Hence, extremely fast operations are not required. It is only recommended not to change the operation in the branches during the evolution of the transient event.



## 7.2 Recommendations

The gas pocket detection method should be verified in a real dendritic wastewater transportation system, which may lead to recommendations on the preferred status of the branch pumping stations, because running branch pumping station may dampen the transient pressures too much.

Once the first gas pocket has been detected, a number of additional simulations can be performed with the estimated gas pocket volume on the first location. The simulated pressure time series can be directly compared with the measured pressure, which may provide more detailed information on the possibility that the gas is distributed over several smaller gas pockets. The predicted gas pocket volume and location may feed an ITA solver as an initial 'educated guess', if more accurate predictions would be required.

Finally, it is recommended to perform a sensitivity analysis with the uncertain parameters, such as the polytropic coefficient, the final gas pocket pressure and the measured frequencies, in order to assess the uncertainty of the predictions.

## 8 Acknowledgements

The authors wish to thank the participants of the CAPWAT project: Gemeentewerken Rotterdam, Waterboard Delfland, Waterboard Hollands Noorderkwartier, Waternet, Waterboard Brabantse Delta, Waterboard Reest en Wieden, Waterboard Rivierenland, Waterboard Zuiderzeeland, Waterboard Fryslân and Waterboard Hollandse Delta, Aquafin, Royal Haskoning, Grontmij Engineering Consultancy, ITT Flygt BV, Foundation Stowa and the Dutch Ministry of Economic Affairs.

## References

Brunone, B. (1999). "Transient test-based technique for leak detection in outfall pipes." Journal of Water Resources Planning and Management **125**(5): 302-306.

Covas, D., Ramos, H., Brunone, B., Young, A. (2004). Leak detection in water trunk mains using transient pressure signals: field tests in Scottish Water. The practical application of surge analysis for design and operation. Chester, BHR Group Ltd.

Deltares (1993 - 2008). WANDA, pipeline simulation software. Delft Hydraulics Software, Deltares | Delft Hydraulics.

Ferrante, M. and B. Brunone (2003). "Pipe system diagnosis and leak detection by unsteady-state tests. 1. Harmonic analysis." Advances in Water Resources **26**(1): 95-105.

Gudmundsson, J. S. a. C., H.K. (1999). Gas-Liquid Metering Using Pressure-Pulse Technology. Annual Technical Conference and Exhibition. Houston, Society of Petroleum Engineers.

Kent (1952). The entrainment of air by water flowing in circular conduits with downgrade slope. Berkeley, California, University of Berkeley. **PhD**.

Liggett, J. A. and L.-C. Chen (1994). "Inverse transient analysis in pipe networks." Journal of Hydraulic Engineering **120**(8): 934-955.

Liou, J. C. P. (1993). Pipeline variable uncertainties and their effects on leak detectability. API Publications. API, American Petroleum Institute: 118.

Lubbers, C. L. (2007). On gas pockets in wastewater pressure mains and their effect on hydraulic performance. Civil engineering and Geosciences. Delft, Delft University of Technology. **PhD**: 290.

Lubbers, C. L., Clemens, F.H.L.R. (2005). On detecting gas pockets in pressurised wastewater mains. 10th Int. Conf. on Urban Drainage. Copenhagen.

Stephens, M., M. Lambert, et al. (2004). Field tests for leakage, air pocket, and discrete blockage detection using inverse transient analysis in water distribution pipes. Proceedings of the 2004 World Water and Environmental Resources Congress: Critical Transitions in Water and Environmental Resources Management.

Stephens, M., Vitkovsky, J., Lambert, M., Simpson, A., Karney, B., Nixon, J. (2004). Transient analysis to assess valve status and topology in pipe networks. The practical application of surge analysis for design and operation. Chester, BHR Group ltd.

Stoianov, I., Maksimovic, C., Graham, N. and Dellow, D. (2003). Field Validation of the Application of Hydraulic Transients for Leak Detection in Transmission Pipelines. International Conference on Computing and Control for the Water Industry. London.

Thorley, A. R. D. (2004). Fluid Transients in Pipeline Systems, A Guide to the Control and Suppression of Fluid Transients in Liquids in Closed Conduits. London, Professional Engineering Publishing Ltd.